Magnetic configuration dependence of turbulent core density fluctuations in Wendelstein 7-X

J.-P. Bähner[1], L. Podavini[2], M. Porkolab[1], A. von Stechow[2], S. K. Hansen[1], E. M. Edlund[3], S. A. Bozhenkov[2], A. Zocco[2], O. Grulke[2,4] and the Wendelstein 7-X Team[2]

[1]*MIT Plasma Science and Fusion Center, Cambridge, MA, USA*

[2]*Max-Planck-Institut für Plasmaphysik, Greifswald, Germany*

[3]*SUNY Cortland, Cortland, NY, USA*

[4]*Technical University of Denmark, Kongens Lyngby, Denmark*

The Wendelstein 7-X (W7-X) stellarator is optimised for reduced neoclassical transport and its confinement is consequently dominated by anomalous transport [1, 2]. Research on stellarator optimisation now moves towards turbulence optimised configurations for future stellarator reactors. In light of this progress, the question of how magnetic geometry affects turbulence and the associated transport in existing optimised experiments such as W7-X should be addressed. The magnetic configuration of W7-X can be varied in different ways, which generally also affects geometric quantities relevant for electrostatic micro-instabilities. This work focuses on the effect of a variation in rotational transform, ι, from the so-called *low iota* to *standard* to *high iota* configuration. Dedicated configuration scans focusing on the plasma edge and magnetic islands in the scrape-off-layer show a very non-linear evolution of the confinement with ι [3]. In this work, we only consider the interplay of core fluctuations with varying configuration. The phase contrast imaging (PCI) diagnostic [4, 5] is one of the main core turbulence diagnostics of W7-X and provides absolutely-calibrated measurements of the line-integrated electron density fluctuations throughout the plasma bulk. The fluctuation amplitude measured by PCI is observed to be affected by the change in ι. Figure 1 shows an overview of fluctuation amplitudes and line-integrated density in a majority of ECRH experiments from the recently concluded experiment campaign, OP2.1. A clear trend of lower fluctuation amplitudes in configurations with higher ι is observed. The ECRH input power ranges from 0.5 MW to 6 MW, showing that the trend is not particular to any power level. The same trend is observed in data from earlier experiment campaigns.

In the latest experiment campaign, dedicated experiments with identical plasma parameters and heating power steps at different density levels were performed in various magnetic configurations. These experiments enable a direct comparison of the three magnetic configurations mentioned above, which consistently shows the same trend as observed in the overview of experiments in figure 1. We focus on a heating power and density combination, which matches the

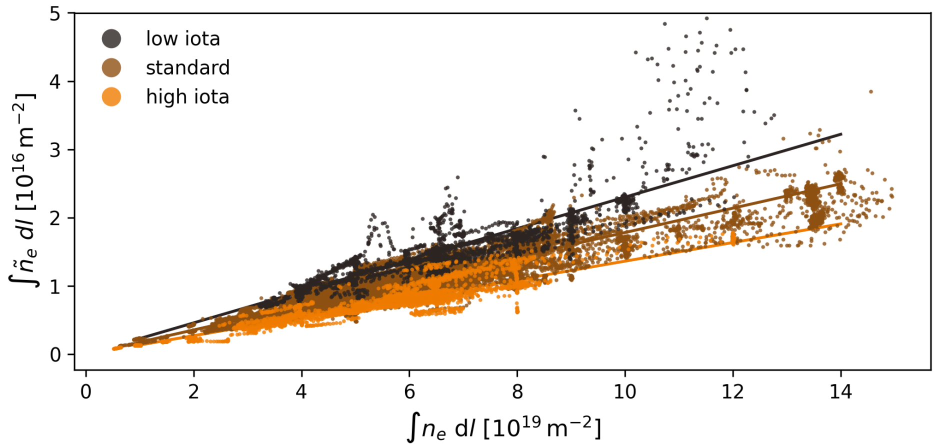

Figure 1: Line-integrated density fluctuation amplitude versus line-integrated density in three magnetic configurations of W7-X with varying rotational transform. Data points represent averages of 100 ms-segments in purely electron-cyclotron-resonance-heated (ECRH) hydrogen plasma with gas-fuelling from the edge. Solid lines represent linear regressions to all data points of one configuration.

experiment scenario previously investigated in the standard (medium iota) configuration [6] but the results presented here apply to other scenarios as well. In the previous study, we found that turbulent fluctuations are dominantly driven by the ion temperature gradient (ITG) mode and are localised in a radial region around $r_{\mathrm{eff}}/a = 0.6 - 0.8$ [6]. By investigating the frequency and wavenumber (roughly poloidal, $\approx k_\theta$) spectra, we find that the difference between the configurations is most obvious for low frequencies and low wavenumbers, which suggests a connection to the ITG drive, since the modes are predominantly destabilised in this regime.

In order to investigate the turbulent drive, gyrokinetic flux tube simulations with kinetic electrons were performed using the code stella [7]. The density and temperature gradients were chosen based on representative kinetic profiles, which were already used in previous studies [6]. Identical gradients were chosen for the three different configurations in order to investigate the isolated effect of magnetic geometry on turbulence. The flux tube crossing the PCI line-of-sight on the outboard side at $r_{\mathrm{eff}}/a = 0.75$ was chosen, also matching the method of the previous study [6]. Results are shown in figure 2. In linear growth rate spectra excluding the electron temperature gradient, a typical ITG peak around $k_y\rho_i = 1$ is observed. The height of the peak differs between the configurations. The difference in growth rate is moderate but reflects the same trend as observed experimentally.[1] Since linear gyrokinetic simulations can qualitatively reproduce

[1]Note that a finite a/L_n and the particular choice of flux tube seems to be important, as a study on saturation via zonal flows in W7-X including simulations in the $\alpha = 0$ flux tube with adiabatic electrons and flat density finds the opposite trend for linear growth rates and nonlinear thermal diffusivity [8].

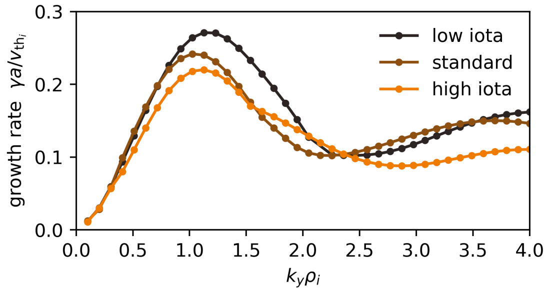

Figure 2: Linear growth rate spectra from gyrokinetic simulations using stella with $a/L_{T_e} = 0$. The main ITG peak around $k_y\rho_i = 1$ shows the same trend as the experimental observations.

the experimentally observed trend based purely on geometric differences, we attempt to identify the corresponding relevant geometric quantities. Figure 3 shows relevant geometric quantities affecting ITG modes along the flux tube crossing the PCI line-of-sight, which was also chosen for the gyrokinetic simulations. Some of these quantities differ only marginally between the configurations at the PCI location, including normal curvature, which drives the toroidal branch of the ITG mode and often sets the mode's structure along the flux tube, as well as flux compression, which increases the real space gradient of the ion temperature and thereby enhances the ITG drive. The quantity showing a significant difference is $|\nabla\alpha|^2$ representing the density of field lines in the binormal direction. At higher values of $|\nabla\alpha|^2$, the finite-Larmor-radius (FLR) effect becomes more relevant, which has a stabilising effect on ITG modes. Configurations with increasing ι exhibit higher values of $|\nabla\alpha|^2$ suggesting that ITG modes are more stable in these configurations, which matches the experimental observations and linear simulation results. It should be mentioned, that the most unstable modes in the linear simulations are not primarily located in the region along the flux tube, where $|\nabla\alpha|^2$ differs the most, due to its stabilising effect. However, a stronger suppression in this region limits the toroidal expansion of the mode and thus its overall growth.

In conclusion, the magnetic geometry of W7-X is observed to affect the amplitude of turbulent density fluctuations. Configurations with higher rotational transform exhibit lower fluctuations. In corresponding linear gyrokinetic simulations, ITG modes show lower growth rates, which qualitatively matches the experimental observations. The effect is expected to originate from increased compression of field lines in the binormal direction leading to more effective FLR suppression. The overall confinement does not seem to be strongly affected by this difference. However, effects on transport and differences in the experimental kinetic profiles between the configurations have not been considered in the present study.

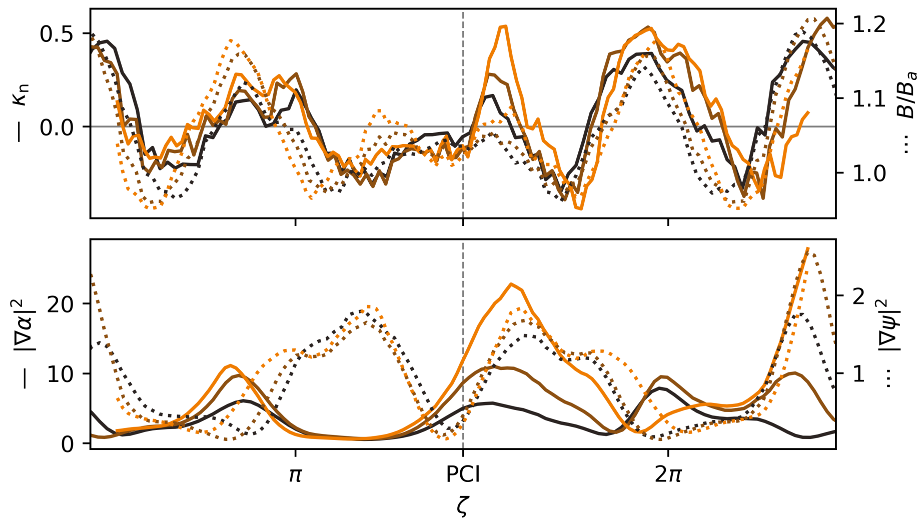

Figure 3: Geometric quantities along the $r_{\rm eff}/a = 0.75$ flux tube crossing the PCI line-of-sight relevant for turbulent micro-instabilities. The quantities represent the normal curvature, $\kappa_{\rm n}$, the magnitude of the magnetic field, B/B_a, the compression of flux surfaces, $|\nabla\psi|^2$, and the compression of field lines within the flux surface, $|\nabla\alpha|^2$, where ψ is the toroidal magnetic flux and α is the Clebsch angle ($\mathbf{B} = \nabla\psi\times\nabla\alpha$). The color coding is identical to figures 1 and 2.

Acknowledgements

Support for the MIT and SUNY-Cortland participation was provided by the US Department of Energy, Office of Fusion Energy Sciences under grant number DE-SC0014229. This work has been carried out within the framework of the EUROfusion Consortium, funded by the European Union via the Euratom Research and Training Programme (Grant Agreement No 101052200 — EUROfusion). Views and opinions expressed are however those of the author(s) only and do not necessarily reflect those of the European Union or the European Commission. Neither the European Union nor the European Commission can be held responsible for them.

References

[1] T. Klinger *et al.* 2019 *Nucl. Fusion* **59** 112004

[2] S. A. Bozhenkov *et al.* 2020 *Nucl. Fusion* **60** 066011

[3] T. Andreeva *et al.* 2022 *Nucl. Fusion* **62** 026032

[4] E. M. Edlund *et al.* 2018 *Rev. Sci. Instrum.* **89** 10E105

[5] Z. Huang *et al.* 2021 *J. Inst.* **16**, P01014

[6] J.-P. Bähner *et al.* 2021 *J. Plasma Phys.* **87** 905870314

[7] M. Barnes, F.I. Parra, M. Landremann 2021 *J. Comput. Phys* **391** 365-380, see also: stella documentation

[8] C. D. Mora Moreno *et al.* 2020 *arXiv:*2009.14750